CellPress
Partner Journal

Molecular Plant
Research Article

Stigma Receptivity Is Controlled by Functionally Redundant MAPK Pathway Components in *Arabidopsis*

Muhammad Jamshed[1,2], Subramanian Sankaranarayanan[1,3], Kumar Abhinandan[1] and Marcus A. Samuel[1,*]

[1]University of Calgary, BI 392, Department of Biological Sciences, 2500 University Dr. NW, Calgary, AB T2N 1N4, Canada

[2]Senior Scientist, Frontier Agri-Science Inc, 98 Ontario Street, Port Hope, ON L1A 2V2, Canada

[3]Department of Botany and Plant Pathology, Purdue University, West Lafayette, IN 47907, USA

***Correspondence: Marcus A. Samuel (msamuel@ucalgary.ca)**

https://doi.org/10.1016/j.molp.2020.08.015

SUMMARY

In angiosperms, the process of pollination relies on species-specific interaction and signaling between the male (pollen) and female (pistil) counterparts where the interplay between several pollen and stigma proteins decides the fate of the pollen. In Brassicaceae, the dry stigmatic papillary cells control pollen germination by releasing resources only to compatible pollen thereby allowing pollen to hydrate and germinate. Despite the identification of a number of stigmatic proteins that facilitate pollination responses, the signaling mechanisms that regulate functions of these proteins have remained unknown. Here, we show that, in *Arabidopsis*, an extremely functionally redundant mitogen-activated protein kinase (MAPK) cascade is required for maintaining stigma receptivity to accept compatible pollen. Our genetic analyses demonstrate that in stigmas, five MAPK kinases (MKKs), MKK1/2/3/7/9 are required to transmit upstream signals to two MPKs, MPK3/4, to mediate compatible pollination. Compromised functions of these five *MKKs* in the quintuple mutant (*mkk1/2/3RNAi/mkk7/9*) phenocopied pollination defects observed in the *mpk4RNAi/mpk3* double mutant. We further show that this MAPK nexus converges on Exo70A1, a previously identified stigma receptivity factor essential for pollination. Given that pollination is the crucial initial step during plant reproduction, understanding the mechanisms that govern successful pollination could lead to development of strategies to improve crop yield.

Key words: reproduction, pollination, stigma receptivity, compatibility, MAPK, redundancy, Exo70A1, exocytosis, phosphorylation

Jamshed M., Sankaranarayanan S., Abhinandan K., and Samuel M.A. (2020). Stigma Receptivity Is Controlled by Functionally Redundant MAPK Pathway Components in *Arabidopsis*. Mol. Plant. **13**, 1582–1593.

INTRODUCTION

Pollination in angiosperms is a highly coordinated process that relies on proper cell–cell communication and signaling between the pollen grain and the stigmatic papillae. In Brassicaceae, the female part of the flower regulates pollination through stigma components called compatibility factors, which are induced as a result of interaction with a suitable mate (pollen) (Doucet et al., 2016). These compatibility factors are proposed to facilitate transport of water and nutrition for pollen hydration, germination, and pollen tube growth (Elleman et al., 1992; Dickinson, 1995; Sankaranarayanan et al., 2015). However, the signaling mechanism behind how these factors are regulated has remained largely unknown. During compatible interactions, calcium spikes and constitutive reactive oxygen species (ROS) accumulation are observed in the stigmas, which most likely can trigger other compatibility factors necessary for pollen growth and germination (Iwano et al., 2004; McInnis et al., 2006; Samuel et al., 2011). There is also precedence for both these second messengers as strong activators of mitogen-activated protein kinases (MAPKs) (Samuel et al., 2000; Cullen and Lockyer, 2002).

MAPK cascade is a highly conserved signaling network in eukaryotes that is involved in signal transduction of inputs from various environmental and developmental stimuli (Xu and Zhang, 2015).

Published by the Molecular Plant Shanghai Editorial Office in association with Cell Press, an imprint of Elsevier Inc., on behalf of CSPB and IPPE, AS.

The MAPK phosphorylation cascade operates in a hierarchical fashion with activated MAPKKK(s) phosphorylating and activating MAPKK(s), which in turn activate MAPK(s) (Rodriguez et al., 2010). In *Arabidopsis*, there are 10 MAPKK(s) (also known as MKKs) and 20 MAPK(s) (commonly known as MPKs), which control numerous cellular responses by regulating different enzymes and transcription factors (Rodriguez et al., 2010). This allows for a staggering number of possible combinations of MKK–MPK pairs with the addition of possible functional redundancy among these proteins. During plant reproduction, various MAPK cascades have been shown to control floral architecture, anther development, ovule development, and pollen tube guidance (Bush and Krysan, 2007; Hord et al., 2008; Wang et al., 2008; Meng et al., 2013; Guan et al., 2014). Despite this, the role of MAPKs during early stages of pollination has not been explored.

Interestingly, mammalian orthologs of TEY class of plant MAPKs, ERK1/2, have been shown to phosphorylate Exo70, a member of exocyst complex, which is involved in exocytosis through tethering, docking, and fusion of secretory vesicles to plasma membrane (Ren and Guo, 2012). This phosphorylation was proposed to promote post-Golgi vesicle transport to plasma membrane to regulate exocytosis along with other cellular processes in response to growth factor signaling (Ren and Guo, 2012). In *Arabidopsis* and canola, Exo70A1 plays an essential role during pollination likely through regulating delivery of vesicles to the plasma membrane required for pollen germination (Samuel et al., 2009).

Given that both calcium and ROS are strong activators of MAPK signaling (Samuel et al., 2000; Cullen and Lockyer, 2002), we predicted that MAPKs will be constitutively active in the stigmatic papillary cells and could play a role during pollination responses. In agreement with our hypothesis, treatment of flowers with a MEK1/2 (MAPKK) inhibitor, U0126 (Favata et al., 1998), previously successfully used to inhibit activation of plant MAPKs (Samuel et al., 2000; Li et al., 2007), caused a significant reduction in compatible pollen attachment and germination (Supplemental Figure 1A and 1B), suggesting the involvement of the MAPK family in regulating pollination. Our genetic analysis of the MAPK pathway components in *Arabidopsis* revealed a functionally redundant MKK–MPK network that converges on Exo70A1 to mediate pollination responses.

RESULTS

MAPKs Are Constitutively Active in Mature Stigmas

While the U0126 inhibitor study provided preliminary evidence for the role for MAPKs in pollination, the challenge was to identify which of the 20 MPKs were involved. We took a biochemical approach using in-gel kinase assays to identify MPKs that are active in the stigmas from stage 12 flowers that undergo anthesis and are primed to accept pollen. When proteins from unpollinated stigmas of stage 12 *Arabidopsis* Col-0 flowers were subjected to in-gel kinase assays, we identified three kinases that were active in mature stigmas (Figure 1A). The masses of these three kinases along with previous evidence with in-gel kinase assays using other *Arabidopsis* tissue types, suggested to us that these three kinases could be MPK3, MPK4, and MPK6 (Wang et al., 2008; Rodriguez et al., 2010). Two of these kinases were validated as MPK6 and MPK3 by using proteins from stigmas of homozygous SALK transfer (T)-DNA mutant lines of *mpk6-2* (SALK_073907) and *mpk3-1* (SALK_151594) where the respective bands were absent (Figure 1A). Since *Arabidopsis mpk4* mutant is a dwarf plant with severe floral defects (Petersen et al., 2000), we suppressed *MPK4* in the stigmas using an RNAi approach utilizing the stigma-specific *SLR1* promoter. Our in-gel kinase assays with stigmatic proteins from *SLR1*::*MPK4Ri* plants validated the identity of the third kinase as MPK4 (Figure 1B).

MPK3 and MPK4 Play a Functionally Redundant Role during Pollination

Given the complexity of the MAPK pathway and the essential nature of MPK3/4/6 for development and cell survival (lethality of *mpk3/6* double mutant and severely dwarfed phenotype of *mpk4*) (Petersen et al., 2000; Wang et al., 2008), we took a genetic approach combined with stigma-specific suppression to address the role of the MAPK cascade during pollination. Since Sincesingle transfer (T)-DNA mutants of *mpk6*, *mpk3-1* or *mpk3-DG*, and *SLR1*::*MPK4Ri* lacked any pollination phenotypes, we created all possible combinations of double mutants and the triple mutant (Figure 1C and Supplemental Figure 2A and Supplemental Table 1). Because of the highly sensitive nature of MAPKs to external stimuli, including touch (Ichimura et al., 2000; Wang et al., 2008), and to keep the perturbation to a minimum, we allowed newly opened flowers to naturally self-pollinate (synchronized with flower opening), followed by assessment of the stigmas for pollination responses through aniline blue staining. As can be observed from Figure 1C, *mpk4Ri*/*mpk6*, *mpk3Ri*/*mpk6*, and *mpk6Ri*/*mpk3* were found to be normal without any change in pollen acceptance (Supplemental Table 1). However, one of the combinations of double mutants *mpk4Ri*/*mpk3 (mpk3-DG)* produced shorter siliques with almost 50% reduction in seeds (Figure 1D and Supplemental Figure 2B). This mutant lacked any floral defects, produced homomorphic flowers, viable pollen, and had efficient transfer of pollen to the stigma (Supplemental Figure 2C–2G). Consistent with the low seed set, *mpk4Ri*/*mpk3* plants showed impaired stigma function when tested for pollination responses (Figure 1E and 1F). After 4 h of pollination, *mpk4Ri*/*mpk3* stigmas displayed severely reduced pollen attachment and germination compared with wild-type Col-0 pistils (Figure 1E and 1F). When stigmas from two independent *mpk4Ri*/*mpk3* lines were assessed for *MPK4* and *MPK3* expression, significantly reduced transcript levels of *MPK4* (RNAi-suppressed) and complete absence of *MPK3* was verified through RT–PCR (Figure 1G; Supplemental Figure 2E). The triple mutant *mpk4Ri*/*mpk6Ri*/*mpk3* also mimicked the phenotype of *mpk4Ri*/*mpk3*, confirming the lack of a role for MPK6 during pollination (Supplemental Figure 3A and 3B). Collectively, our observations indicate that MPK3 and MPK4 are a functionally redundant pair of MAPKs required for mediating stigma receptivity.

Five MKKs (MKK1/2/3/7/9) Are Required for Pollination Responses

We next investigated which of the 10 upstream MKKs were necessary to transmit the signal to MPK3/4 to control pollination.

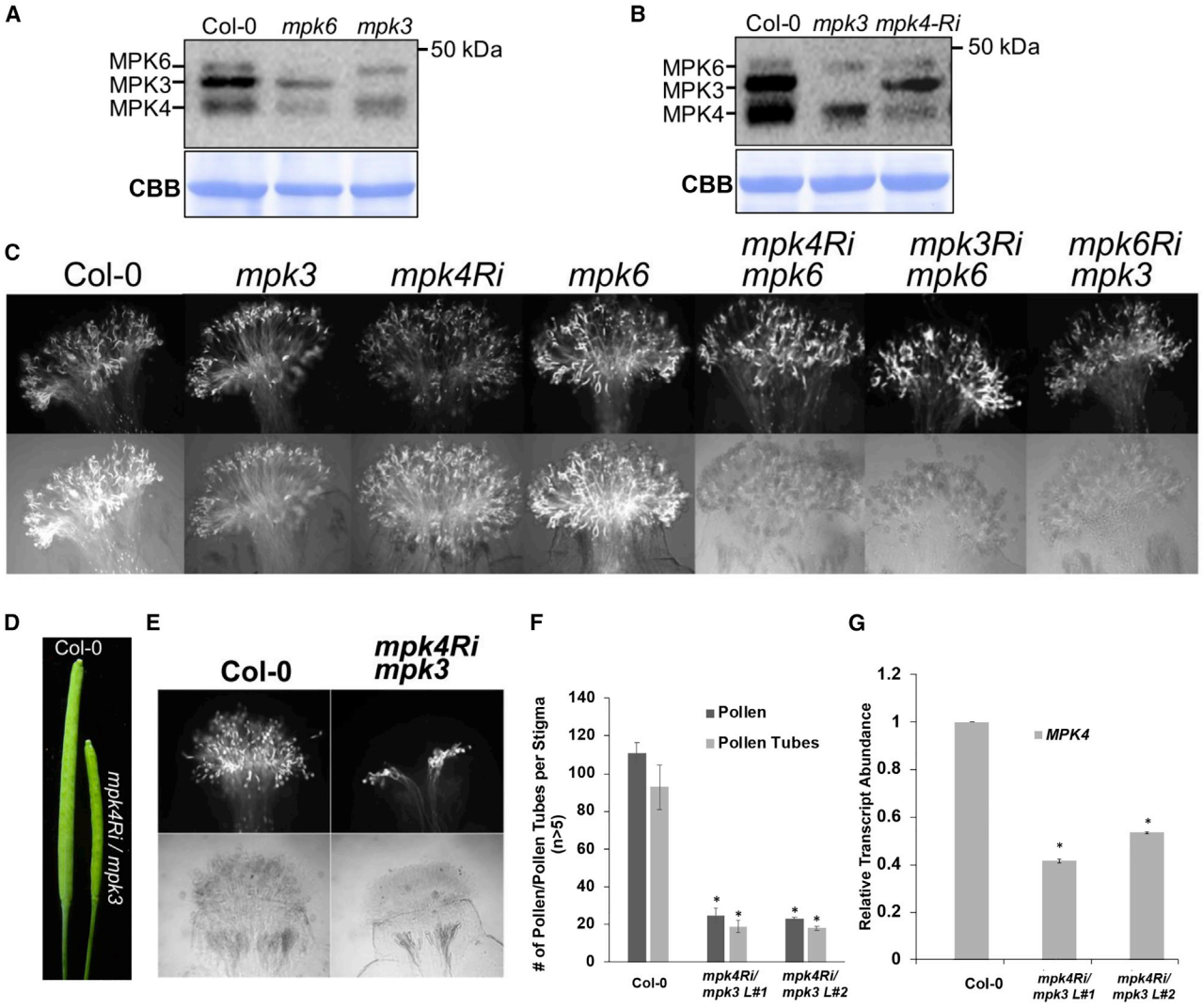

Figure 1. Loss of MPK3 and MPK4 Results in Reduced Compatibility.

(A) In-gel kinase assays show activity of MPK3 and MPK6 in Col-0, *mpk3*, and *mpk6* mutant in stage 12 stigmas. The lower panel shows CBB staining of a parallel gel showing protein loading. **(B)** In-gel kinase assay showing activity of MPK4 and MPK3 in Col-0, *mpk3*, and *mpk4 RNAi* stage 12 stigmas. The lower panel shows CBB staining of a parallel gel showing protein loading. **(C)** Aniline blue assays of stigmas from various MAPK single and digenic mutants showing pollen and pollen tubes after self-pollination. All stigmas were allowed to naturally pollinate and collected 4 h after flower opening. All RNAi constructs were placed under a stigma-specific *SLR1* promoter.

(D) Siliques of Col-0 and *mpk4Ri*/*mpk3* mutant showing reduced seed set.

(E) Aniline blue assays of pollinated stigmas from Col-0 and *mpk4Ri*/*mpk3* mutant.

(F) Average number of pollen attached, and pollen tubes germinated in Col-0 and *mpk4Ri*/*mpk3* mutant ($n > 5$). Error bars represent ±SE. Asterisks represent values significantly different from Col-0 at $P < 0.05$.

(G) qPCR analysis showing relative transcript abundance of *MPK4* in stigmas from stage 12 flowers of Col-0 and two independent *mpk4Ri*/*mpk3* mutant lines ($n = 3$). Error bars indicate ±SE. Asterisks indicate significant differences (*$P < 0.05$).

For this, we used a targeted genetic approach to circumvent lethality associated with loss of some of these kinase combinations (both *mkk1/2* and *mkk4/5* digenic mutants are known to be lethal) (Wang et al., 2007; Kong et al., 2012). Based on previous large-scale yeast two-hybrid and protein array data, eight MKKs (MKK1-6, 7, and 9) have the ability to interact or activate either MPK3 or MPK4 or both (Jin et al., 2008; Popescu et al., 2009). We did not include MKK6 in the screen because it is primarily known to be involved during cytokinesis (Takahashi et al., 2010). As shown in Figure 2A, Supplemental Figures 4–6, all possible combinations (single, double, triple, quadruple, and quintuple) of these kinases were created followed by assessment of T1 and T2 generations for plants that phenocopied *mpk4Ri*/*mpk3* pollination phenotype (Supplemental Table 2). For the combinatorial transgenics, the double *mkk7*/*mkk9* null mutant was used in combination with various stigma-specific RNAi constructs to specifically suppress a subset of *MKKs* in the stigmas. Of all the combinations tested, one of the quintuple mutants, *mkk1/2/3Ri*/*mkk7/9*, in which *MKK1/2/3* were suppressed in the stigmas of *mkk7/9* null

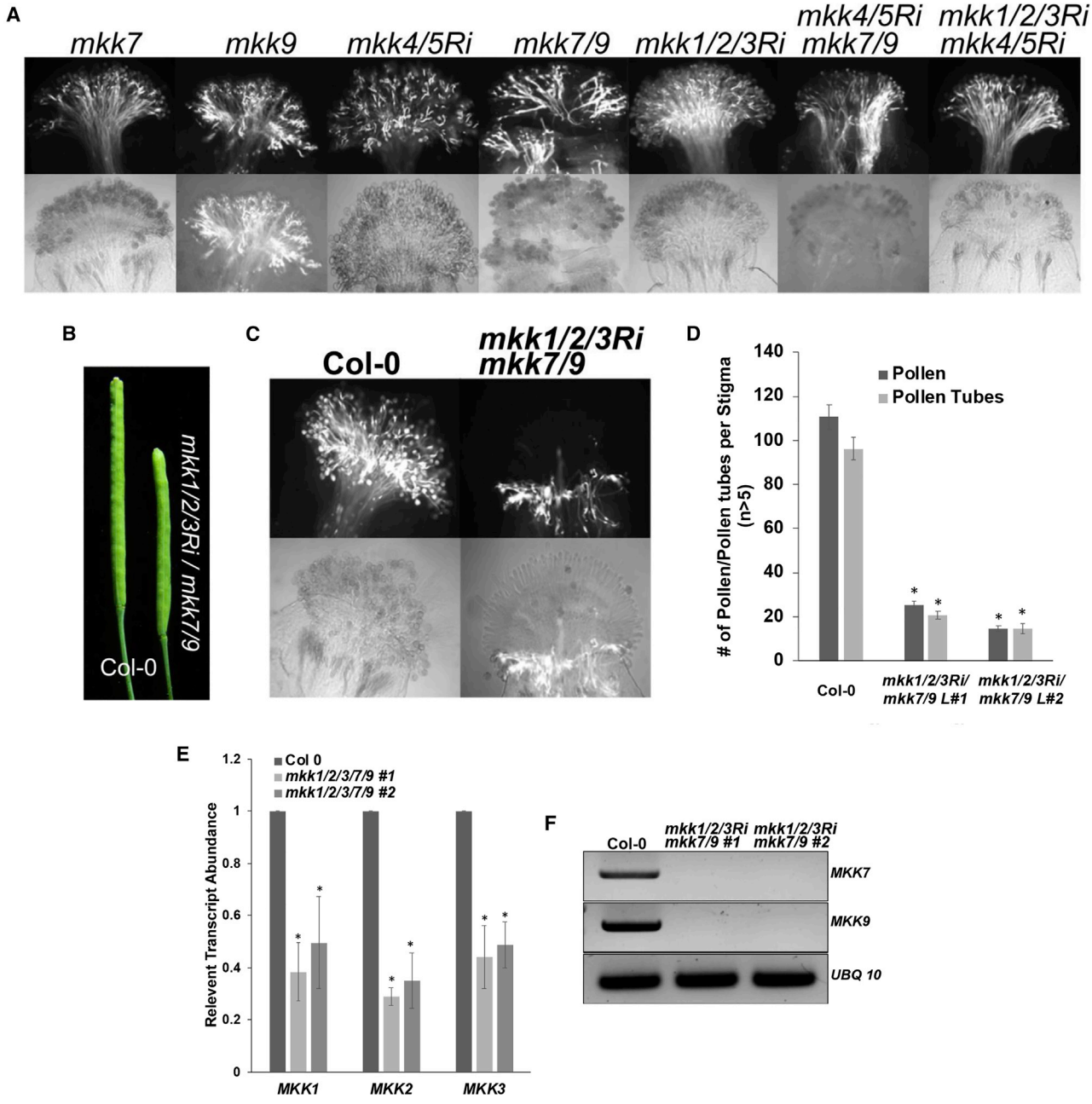

Figure 2. Five MKKs Regulate Compatible Pollination.

(A) Aniline blue assays of stigmas from various *MKK* single and combinatorial mutants showing pollen attachment and pollen tube growth after self-pollination. All stigmas were allowed to naturally pollinate and collected 4 h after flower opening. All RNAi constructs were placed under a stigma-specific *SLR1* promoter.

(B) Siliques of Col-0 and *mkk1/2/3Ri/mkk7/9* mutant showing reduced seed set.

(C) Aniline blue assays of pollinated stigmas from Col-0 and *mkk1/2/3Ri/mkk7/9* mutant showing pollen and pollen tubes.

(D) Average number of pollen attached, and pollen tubes germinated in Col-0 and *mkk1/2/3Ri/mkk7/9* mutant ($n > 5$). Error bars show ±SE. Asterisks indicate significant differences (*$P < 0.05$).

(E) qPCR analysis showing relative transcript abundance of *MKK1*, *2*, and *3* in stigmas from stage 12 flowers of Col-0 and two independent *mkk1/2/3Ri/mkk7/9* mutant lines ($n = 3$). Error bars indicate ±SE. Asterisks indicate significant differences (*$P < 0.05$).

(F) RT–PCR analysis showing lack of *MKK7* and *MKK9* in the *mkk1/2/3Ri/mkk7/9* mutant lines.

mutant background, displayed pollination and fertility defects similar to *mpk4Ri/mpk3* (Figure 2B–2D and Supplemental Figure 5A). This quintuple mutant did not display any floral phenotypes, produced homomorphic flowers with normal anther dehiscence, viable pollen and unimpaired pollen transfer on to stigmas (Supplemental Figure 5B–5E). Suppression of *MKK1/2/3* was confirmed in mature stigmas of two independent quintuple mutant lines through qPCR and absence

of *MKK7/9* was verified through RT–PCR (Figure 2E and 2F). In *mkk1/2/3Ri/mkk7/9* line, suppression of *MKK3* was required to confer a phenotype identical to *mpk3/4* as the quadruple *mkk1/2Ri/mkk7/9* plants showed only moderate pollination defects, while the rest of the multi-locus mutants were fully fertile exhibiting no pollination anomalies (Supplemental Figures 4 and 6A–6F; Supplemental Table 2). This was not surprising, as MKK3 has been previously shown to activate MPK3 and MPK4 (Popescu et al., 2009).

Activated MPK3 and MPK4 Can Phosphorylate the "SP" Motif of Exo70A1

Having established that MAPK signaling is required for compatible pollination to occur, we next focused on how MAPK signaling is integrated to regulate stigmatic factors required for pollen acceptance. One of the compatibility factors that has been shown to play a central role in stigma receptivity is Exo70A1, a member of the exocyst complex (Samuel et al., 2009). Loss of *Exo70A1* resulted in inability of stigmas to support pollen hydration and germination (Samuel et al., 2009). Protein sequence analysis of Exo70A1 revealed a single consensus MAPK phosphorylation (SP) motif with a docking domain upstream of the SP motif (Supplemental Figure 7). To test, if activated MPK4 can phosphorylate serine 328 of the SP motif of Exo70A1, full-length recombinant glutathione S-transferase (GST)-Exo70A1 and GST-Exo70A1 (S328A) proteins were incubated with recombinant 6×HIS-MPK4 along with constitutively active GST-MKK1 (CAKK1) in the presence of radioactive γ-^{32}P (Figure 3A). Strong phosphorylation of GST-Exo70A1 was observed in the presence of 6×HIS-MPK4 and GST-CAKK1 and only marginal background phosphorylation was observed with GST-Exo70A1 (S328A) (Figure 3A). To unequivocally demonstrate that serine 328 of Exo70A1 is phosphorylated by activated upstream MPK3/4, we obtained synthesized short peptides comprising of residues of 323–335 (AR***S***KR***S***PEKLFVL and AR***S***KR***A***PEKLFVL) with either an intact S328 residue or S328 mutated to an alanine and subjected them to *in-vitro* phosphorylation assays. These peptides were immobilized on polyvinylidene fluoride (PVDF) membrane and subjected to *in-vitro* phosphorylation assays using activated 6×HIS-MPK4 (activated with GST-CAKK1) followed by immunoblotting with anti-phosphoserine antibodies (Figure 3B). We observed that the synthetic peptide with an intact SP motif was exclusively phosphorylated by activated MPK4 while the mutated S328A peptide was not detected by the phospho-serine antibodies (Figure 3B). The results clearly demonstrate that MPK4 can specifically phosphorylate serine 328 of Exo70A1 (Figure 3B). Similar SP-specific phosphorylation was also observed with activated MPK3 protein (Supplemental Figure 8).

Exo70A1 Serine 328 of SP Motif Is Required for Successful Pollination

To further characterize whether this MAPK-mediated phosphorylation of serine 328 of Exo70A1 is needed for its function in pollination, we used complementation assays to transform *exo70A1-1* with either *35S::YFP-Exo70A1(WT)* or *35S::YFP-Exo70A1(S328A)*. For complementation studies, due to the developmental and reproductive defects observed in *exo70A1-1*$^{-/-}$ (Synek et al., 2006), we transformed heterozygous lines (*exo70A1-1*$^{+/-}$), followed by screening for T1 transformants that were homozygous for *exo70A1-1*$^{-/-}$ that harbored the transgene. These transgenic lines in the T1 generation *exo70A1-1*$^{-/-}$ background were recovered at very low frequency. As expected, the wild-type *35S::YFP-Exo70A1(WT)* fully rescued the *exo70A1-1* pollination defects and other associated whole-plant developmental phenotypes (Figure 3C–3E and Supplemental Figure 9). In contrast, *35S::YFP-Exo70A1(S328A)* was incapable of rescuing any of the *exo70A1-1* phenotypes (Figure 3C–3E and Supplemental Figure 9). The *35S::YFP-Exo70A1(S328A)/exo70A1-1* lines were phenotypically similar to *exo70A1-1* plants, having a dwarf phenotype with distinctly shorter stigmatic papillae than Col-0, affected in pollen acceptance and produced shorter siliques (Figure 3C–3E and Supplemental Figures 9 and 10A). This strongly indicated that S328 is necessary for Exo70A1 function. To discern whether the presence of serine 328 or its phosphorylation was necessary for full functionality of Exo70A1, we complemented *exo70A1-1* mutant with *35S::YFP-Exo70A1(S328D)*, a phosphomimic version of Exo70A1 (Figure 3C–3E and Supplemental Figure 10B). The Exo70A1 phosphomimic was able to almost fully rescue all developmental and pollination phenotypes, further validating the requirement of S328 phosphorylation for Exo70A1 function (Supplemental Figures 9 and 10B and Figure 3C–3E).

Serine 328 of Exo70A1 Is Required for Plasma Membrane Localization of Exo70A1

Exo70A1 is known to localize to the plasma membrane in stigmatic papillae and also in root epidermal cells (Samuel et al., 2009; Drdová et al., 2013; Fendrych et al., 2013; Wu et al., 2017). To examine the role of S328 phosphorylation on Exo70A1 localization, we observed localization of YFP-tagged versions of Exo70A1 in *exo70A1-1* background (Figure 4A–4D). Stigmas from stage 12 flowers of these transgenics were whole mounted and subjected to confocal microscopy both under laser scanning to detect YFP (Supplemental Figure 11) as well as bright-field imaging (Supplemental Figure 12). In unpollinated stigmas, YFP-Exo70A1(WT) localized to the plasma membrane as reported previously (Samuel et al., 2009) (Figure 4B and Supplemental Figure 11). However, YFP-Exo70A1 (S328A) failed to localize to the plasma membrane and was found diffused throughout the cytoplasm (Figure 4C) and at times in vesicular structures (Supplemental Figures 11 and 13A) in the shorter papillary cells of *YFP-Exo70A1(S328A)/exo70A1-1* lines. The lack of plasma membrane localization suggested that S328A mutation likely caused an aberration in trafficking and impaired its ability to localize at the plasma membrane where Exo70A1 controls exocytosis. This localization defect observed with the YFP-Exo70A1(S328A) was fully rescued by the YFP-Exo70A1(S328D) phosphomimic (Figure 4D and Supplemental Figure 11). The similarity in localization between Exo70A1(WT) and Exo70A1(S328D) suggests that phosphorylation of Exo70A1 at S328 is likely a necessary event for membrane localization of Exo70A1, where it can regulate exocytosis.

Phosphomimic Exo70A1(S328D) Rescues *mpk4Ri/mpk3* Phenotype

To unequivocally confirm that Exo70A1 phosphorylation is necessary downstream of MPK3/4 activation, we transformed *mpk4Ri(stigma-specific)/mpk3* lines with either *Exo70A1(WT)-RFP* or the phosphomimic version *Exo70A1(S328D)-RFP*

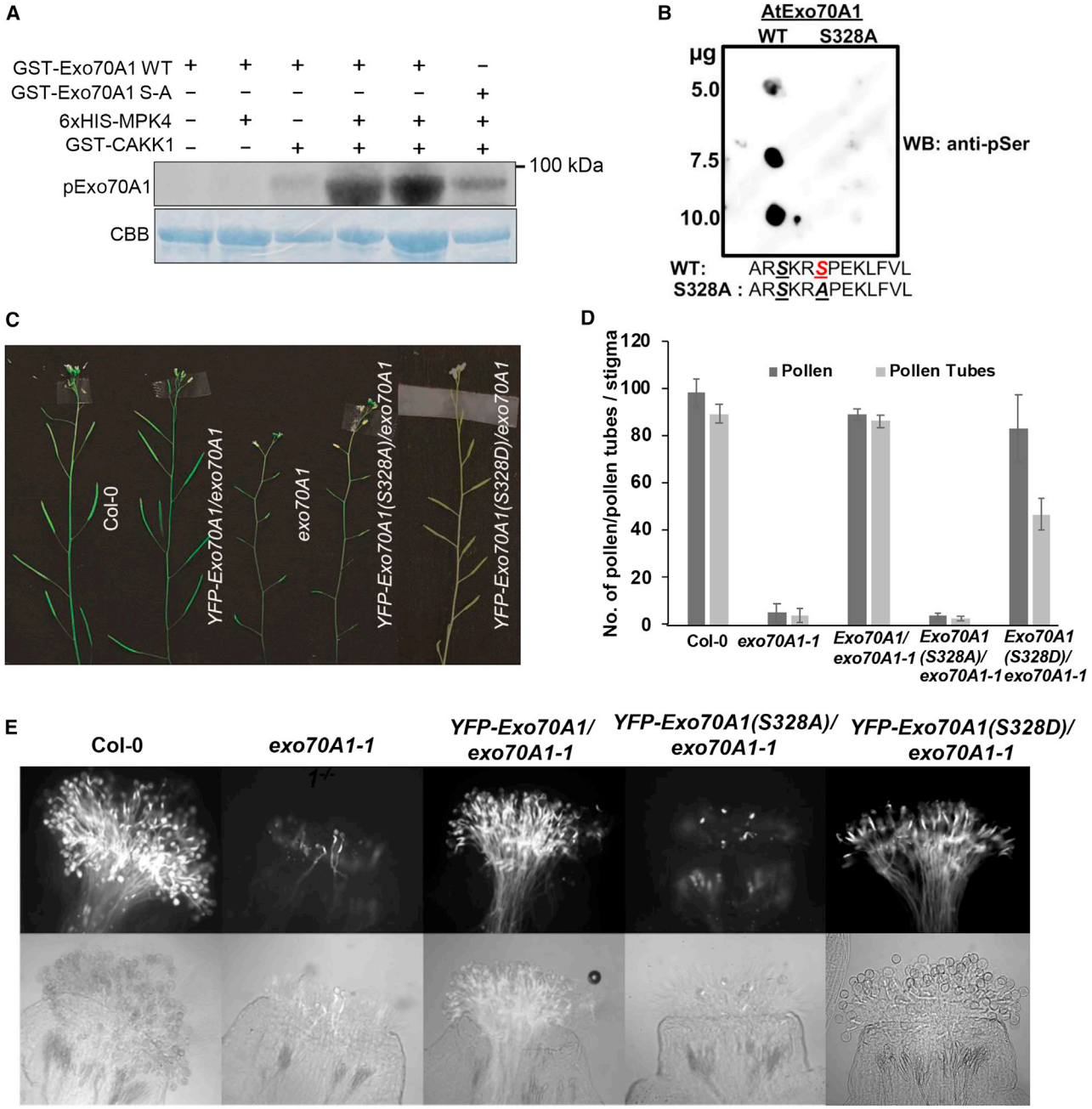

Figure 3. Phosphorylation of Exo70A1 Is Required for Compatible Pollination.

(A) *In vitro* kinase assay showing phosphorylation of GST-Exo70A1 by 6×HIS-MPK4. Lanes 4 and 5 contain 5 and 10 µg of Exo70A1, respectively.

(B) Dot blot showing the phosphorylation of wild type (WT) Exo70A1 peptide (residues 323–335) blotted in various concentrations. Kinase reaction was performed in the presence of pre-activated 6×HIS-MPK4 with GST CAKK1 and blotted with anti-pSer antibody.

(C) Inflorescence phenotype of Col-0, *35S*::*YFP-Exo70A1(WT)/exo70A1*,*exo70A1*,*35S*::*YFPExo70A1(S328A)/exo70A1* (line 2) and *35S*::*YFP-Exo70A1(S328D)/exo70A1* (line 41).

(D) Average number of pollen attached, and pollen tubes germinated on stigmas of these lines. Error bars indicate ±SE ($n > 5$). Asterisks indicate significant differences (*$P < 0.05$).

(E) Aniline blue images of pollinated stigmas from respective WT, mutant, and complemented lines.

and assessed the T1 transformants for their ability to rescue the pollination defects. *35S*::*Exo70A1(WT)-RFP/mpk4Ri/mpk3* exhibited fertility defects similar to *mpk4Ri/mpk3* mutant with reduced seed set, pollen attachment, and germination comparable with *mpk4Ri/mpk3* (Figure 5A–5D). In contrast, the phosphomimic version *35S*::*Exo70A1(S328D)-RFP/mpk4Ri/mpk3* fully complemented the pollination defects and led to seed set, pollen attachment, and germination similar to Col-0 (Figure 5A and 5B, 5E, and 5F). Our observations further validate the requirement of

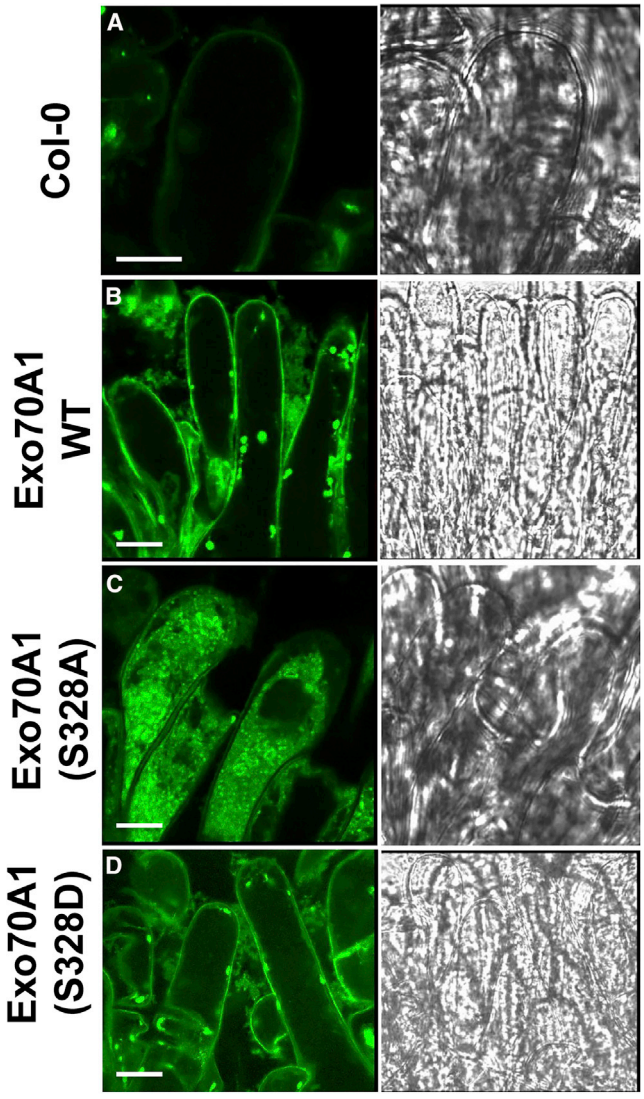

Figure 4. Disruption of Exo70A1 MAPK Phosphorylation Motif Impairs Its Membrane Localization

Confocal imaging of stage 12 papillary cells from Col-0 **(A)**, *35S::YFP-Exo70A1(WT)/exo70A1* **(B)**, *35S::YFP-Exo70A1(S328A)/exo70A1 (line 2)* **(C)**, and *35S::YFP-Exo70A1(S328D)/exo70A1 (line 41)* **(D)**. Membrane localization was changed to diffused and cytosolic in *35S::YFP-Exo70A1(S328A)/exo70A1* mutant, whereas phosphomimic version 35S::YFP-Exo70A1(S328D)/exo70A1 restores the plasma membrane localization. The left column shows zoomed-in images of papillary cells, the right column shows bright-field images of same papillary cells. Scale bar corresponds to 5 μm.

phosphorylation of serine 328 by upstream MPKs for successful pollination.

DISCUSSION

Through this study, we were able to show that a subset of functionally redundant MAPK pathway components converges on the receptivity factor Exo70A1 to mediate stigma receptivity. Although the in-gel kinase assays detected three MAPKs, MPK3, MPK4, and MPK6 that were constitutively active in stage 12 stigmas of *Arabidopsis*, mutational analysis revealed that only MPK3 and MPK4 were required for pollination responses to occur. The loss of these two proteins resulted in severe reduction in pollen germination and pollen tube growth despite having homomorphic flowers that were unaffected in pollen transfer to the stigmas. Our assays had to rely on natural pollination as MAPKs are quite sensitive to manipulation and we were also utilizing the stigma-specific RNAi-mediated suppression of *MPK4* to circumvent lethality or severe phenotypes associated with the double knockout mutants (Petersen et al., 2000; Ichimura et al., 2002; Frei dit Frey et al., 2014). Given that all these three kinases are commonly associated with defense against pathogens (McInnis et al., 2006; Gao et al., 2008; Pitzschke et al., 2009; Galletti et al., 2011; Kong et al., 2012), we predict that one of the major roles of these kinases could be to protect the reproductive tissues from invading pathogens while simultaneously promoting stigma receptivity to compatible pollen. The constitutive accumulation of ROS in mature stigmas (McInnis et al., 2006) suggests that ROS might be a candidate upstream signal as they are known to activate these kinases (Kovtun et al., 2000; Desikan et al., 2001).

We have identified that the MPK3/4 duo is regulated by five upstream MKKs. Loss of function of MKK7/9 simultaneously with suppression of MKK1, MKK2, and MKK3 in the *mkk1/2/3Ri/mkk7/9* quintuple mutant led to reduced pollen attachment and the mutant phenocopied the *mpk4Ri/mpk3* pollination phenotype. The extreme functional redundancy observed at the MKK tier in facilitating stigma receptivity is certainly a paradigm shift in plant MAPK signaling where it is believed that fewer MKKs regulate all the MPKs (Wang et al., 2007; Sung et al., 2008; Popescu et al., 2009; Sun et al., 2018; Zhang et al., 2020). Although most of the MKKs can interact with multiple downstream MPKs (Jin et al., 2008), this does not preclude the possibility of the opposite where multiple MKKs can control activity of a selected smaller subset of MPKs under certain conditions or in a specific tissue, such as the stigmatic papillary cells. It is also plausible that, since MPK3 and MPK4 belong to subgroups A and B, respectively (Ichimura et al., 2002), an increased number of MKKs could interact with these kinases to influence stigma receptivity.

We have been able to show that the activated MPK3/4 pair converges on Exo70A1, a receptivity factor that regulates pollen hydration and germination in both *Brassica* and *Arabidopsis* (Samuel et al., 2009; Safavian and Goring, 2013). Both MPK3 and MPK4 phosphorylate Exo70A1 at the consensus 'SP' motif and this phosphorylation is essential to maintain stigma receptivity (Figure 3). A similar scenario has been observed in mammalian cells where ERK1/2-dependent phosphorylation of Exo70 was shown to facilitate interaction of Exo70 with other exocyst subunits to promote exocytosis in response to growth factor signaling (Ren and Guo, 2012). Both MPK3 and MPK4 also have TEY phosphorylation residues in their activation loop and belong to the ERK1/2 class of mammalian kinases (Dóczi et al., 2012). Mutation in the consensus phosphorylation motif of Exo70A1(S328A) disrupted its localization and was incapable of rescuing any of the *exo70A1-1* defects (Figure 3). To ascertain that lack of Exo70A1(S328A) protein stability was not the reason for the observed inability to rescue *exo70A1-1* defects, the stability of Exo70A1(S328A) was also confirmed through western blotting to detect fluorescently tagged

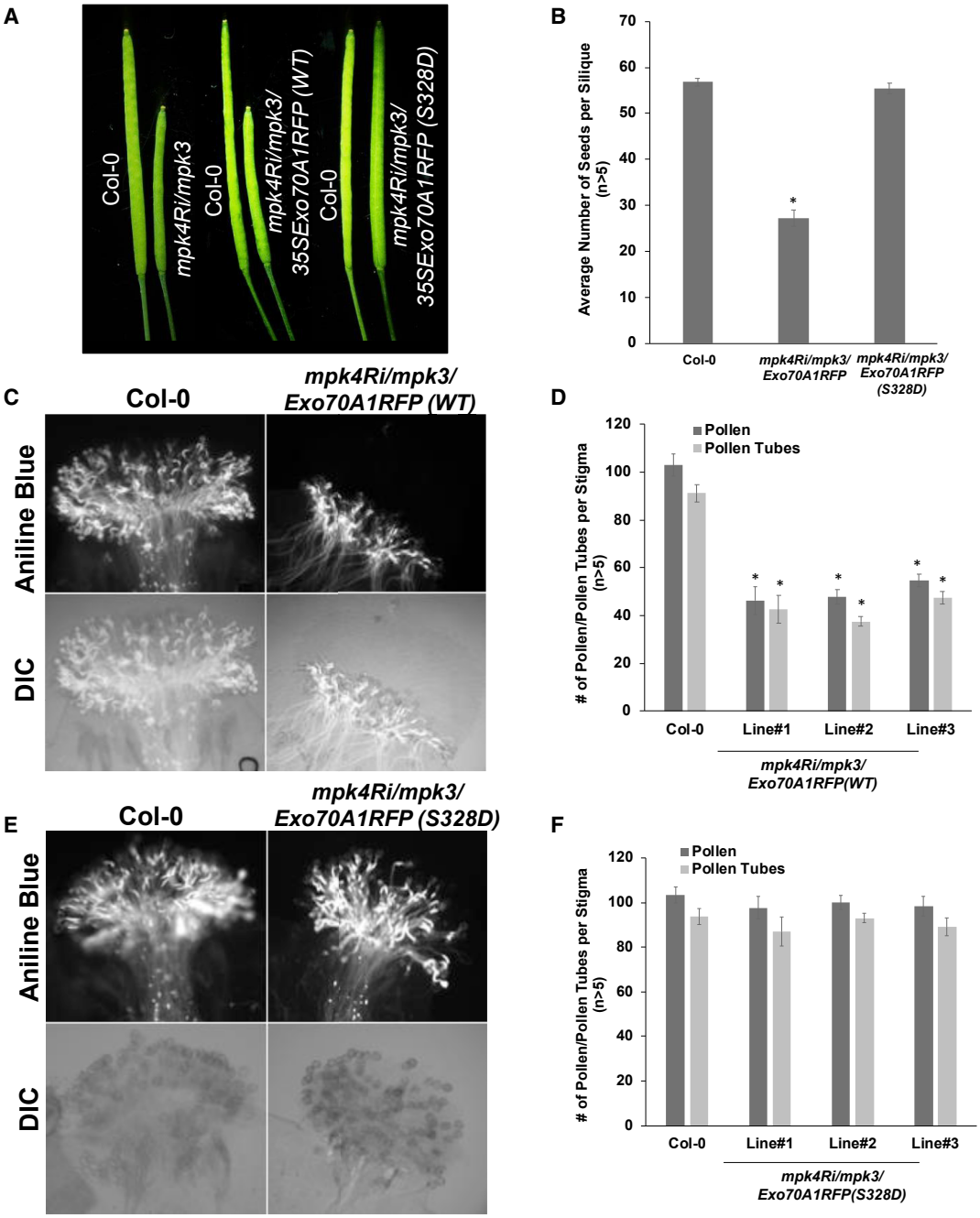

Figure 5. Phosphomimic Version of Exo70A1 Rescues *mpk4Ri/mpk3* Pollination Defects.

(A) Siliques from Col-0, *mpk4Ri/mpk3*, *35SExo70A1RFP(WT)/mpk4Ri/mpk3*, and *35SExo70A1RFP(S328D)/mpk4Ri/mpk3* showing that the phosphomimic version of Exo70A1 can rescue the *mpk4Ri/mpk3* phenotype.

(B) Graph representing the average number of seeds per silique in respective phenotypes. Error bars indicate ±SE (n = 5). Asterisks show values are significantly different from Col-0 at $P < 0.05$.

(C) Aniline blue images of pollinated (4 h) stigmas of Col-0 and *mpk4Ri/mpk3/35SExo70A1RFP(WT)* line 3 showing attached pollen and germinated pollen tubes.

(D) Average number of pollen attached and pollen tubes germinated on stigmas of Col-0 and the independent *mpk4Ri/mpk3/35SExo70A1RFP(WT)* transgenic lines. Error bars represents ±SE (n = 5). Asterisks show values are significantly different from Col-0 at $P < 0.05$.

(E) Aniline blue images of pollinated (4 h) stigmas of Col-0 and *mpk4Ri/mpk3/35SExo70A1RFP(S328D)* line 2 showing attached pollen and germinated pollen tubes.

(F) Graph representing average number of pollen attached and pollen tubes germinated on stigmas of stigmas of Col-0 and the independent *mpk4Ri/mpk3/35SExo70A1RFP(S328D)* transgenic lines. Error bars represent ±SE (n = 5).

versions of Exo70A1(S328A) in both *exo70A1* and Col-0 backgrounds (Supplemental Figure 13B and 13C).

Our phenotypic observations with the phosphodeficient Exo70A1(S328A) and the phosphomimic Exo70A1(S328D) clearly indicate the requirement of phosphorylation of serine 328 for full functionality of Exo70A1 (Figure 3 and Supplemental Figure 9). This is not limited to the papillary cells, as the dwarf phenotype of *exo70A1* was also not rescued in the *YFP-Exo70A1(S328A)/exo70A1-1* lines (Supplemental Figure 9). Although this study has focused on the role of Exo70A1 and its phosphorylation during stigmatic receptivity, it is critical to note that the serine 328 phosphorylation of Exo70A1 is essential for its function and likely the secretory processes regulated by the exocyst complex throughout the plant (Supplemental Figure 9). Very similar to our observations, Exo70(S250A) could not stimulate exocytosis in mammalian cells, while the phosphomimic was sufficient to rescue this defect (Ren and Guo, 2012). In *Arabidopsis*, mutating the MPK3/6-specific MAPK phosphorylation motif of the transcription factor, SPEECHLESS has been shown to cause over-proliferation of stomata (Lampard et al., 2008). In metastatic melanoma cells, it was demonstrated that BRAF with V600E mutation causes constitutive activation of RAF–MEK–ERK pathways that converge on Exo70 phosphorylation, leading to actin dynamics and secretion of matrix metalloproteases (Lu et al., 2016).

Although there are 23 paralogs in *Arabidopsis*, Exo70A1 is highly related to other eukaryotic Exo70s involved in exocytosis (Synek et al., 2006). Loss of function of Exo70A1 alone can cause a dwarf phenotype along with shorter, non-receptive stigmatic papillae (Synek et al., 2006; Samuel et al., 2009). Through an RNAi approach, each of the subunits of the complete octomeric complex was also shown to be required for conferring stigma receptivity, further validating the role of exocytosis as a crucial process during pollen acceptance (Safavian et al., 2015). Exocyst subunits are known to dock at the plasma membrane and create sites for vesicle tethering, and Exo70A1 is also required for plasma membrane localization of other subunits, such as Sec6 (Fendrych et al., 2013). The lack of plasma membrane localization of Exo70A1 in the absence of S328 phosphorylation suggests that phosphorylation could result in interaction of Exo70A1 with other subunits to traffic to the plasma membrane where it can regulate exocytosis. Alternatively, phosphorylation of Exo70A1 could recruit it to the membrane where it allows the assembly of the exocyst complex by associating with other subunits to facilitate vesicle tethering and exocytosis. Consistent with this, loss of function of Exo70A1 in *Arabidopsis* and *Brassica napus* resulted in accumulation of these vesicles in the cytoplasm of both unpollinated and pollinated papillary cells (Safavian and Goring, 2013). Accumulation of these vesicles in the cytoplasm is proposed to restrict the necessary resources from being delivered to the germinating pollen (Safavian and Goring, 2013).

Collectively, we have been able to unravel a novel role for MAPK signaling during pollination that converges on a key regulator of the stigmatic exocytotic pathway essential for stigma receptivity (Figure 6). The extreme functional redundancy observed at the MKK level of the cascade breaks the current paradigm where a smaller number of MKKs are believed to regulate a large class of MPKs, suggesting that size of gene family may not necessarily correlate with overlapping functions. Given the agronomic importance of various crop plants that belong to Brassicaceae, understanding the signaling mechanism during compatible pollination responses could lead to developing strategies to improve crop yield.

MATERIALS AND METHODS

Plant Materials and Growth Conditions

Arabidopsis thaliana Col-0 ecotype was used as wild type. Mutant alleles of *mpk3* (SALK_151594), *mpk6* (SALK_073907), *mkk7* (SM_CS110477), *mkk9* (SAIL_60_H_06), and *exo70A1-1* (SALK_014826) were obtained from ABRC and homozygous lines were isolated. One of the single mutant *mpk3-DG* (Miles et al., 2005) was obtained from Dr. Brian Ellis (University of British Columbia, Vancouver, Canada). All seeds were surface sterilized and plated on 0.5× MS, 1% sucrose, and 0.7% phytagar, stratified for 3–5 days at 4°C in dark and germinated in plant growth incubators. The seedlings were then transplanted to soil and plants were maintained in growth chambers at 22°C with a 16 h/8 h (light/dark) cycle and a light intensity of 120 μmol m^{-2} s^{-1} 7 days.

RNAi Constructs and Generation of Multi-Locus Mutants

RNAi constructs of *MPK3*, *MPK4*, and *MPK6* were generated using the first 600 bases of the open reading frame (ORF) as described previously (Samuel et al., 2009). Infusion cloning (Clontech) was used to introduce these RNAi constructs into modified pBin19 binary vector containing stigma-specific *SLR1* promoter, to drive suppression of these genes exclusively in the stigmatic tissue. The primers used for developing RNAi constructs are shown in Supplemental Table 3. For generating RNAi constructs of *MKKs*, tandem constructs of *MKK1/2*, *MKK1/2/3*, and *MKK4/5*, were synthesized (GenScript, Piscataway, NJ, USA), using the first 200–300 bases of the ORF of each gene. These constructs were then utilized for building tandem RNAi constructs of *MKK1/2*, *MKK1/2/3*, and *MKK4/5* through infusion cloning in pBin19 vector (for primers refer to Supplemental Table 3). *AtExo70A1* ORF was amplified and cloned in pGEX4T-1. Site directed mutagenesis was used to change serine 328 to alanine (S328A) and aspartic acid (S328D) by quick change PCR (Invitrogen). Clones were sequenced to confirm the changes and absence of mismatches. *Exo70A1*, *Exo70A1(S328A)*, and *Exo70A1(S328D)* were PCR amplified and cloned as a C-terminal fusion with *YFP* in pCAMBIA 1301 vector to generate *35S*::*YFP-Exo70A1*, *35S*::*YFP-Exo70A1(S328A)*, and *35S*::*YFP-Exo70A1(S328D)* constructs. Primers used for generating these constructs are shown in Supplemental Table 4. Col-0 and other mutant plants were transformed using *Agrobacterium tumefaciens* (GV3101)-mediated transformation using the floral dip method (Clough and Bent, 1998). Transformant selection was performed by screening on 0.5× MS, 1 % sucrose plates containing either hygromycin (25 mg/l) or kanamycin (50 mg/l). Putative transformants were then transplanted to soil, maintained in growth chambers, and subjected to further analysis.

Recombinant Protein Production and Purification

GST fusion clones of *CAKK1* and *CAKK7* were obtained from Dr. Brian Ellis (University of British Columbia, Vancouver, Canada). MPK3 and MPK4 ORFs were cloned under 6×HIS tag in pET15b vector. All recombinant GST fusion and 6×HIS proteins were expressed in *Escherichia coli* BL21 cells. Cultures were induced with either 0.01 or 0.1 mM isopropylthio-galactoside for 6 h at 30°C, followed by purification according to the manufacturer's protocol (Sigma-Aldrich).

In-Gel Kinase Assay

In-gel kinase assays were performed as described earlier (Samuel et al., 2000). Stage 12 stigmas from the various genotypes were collected in

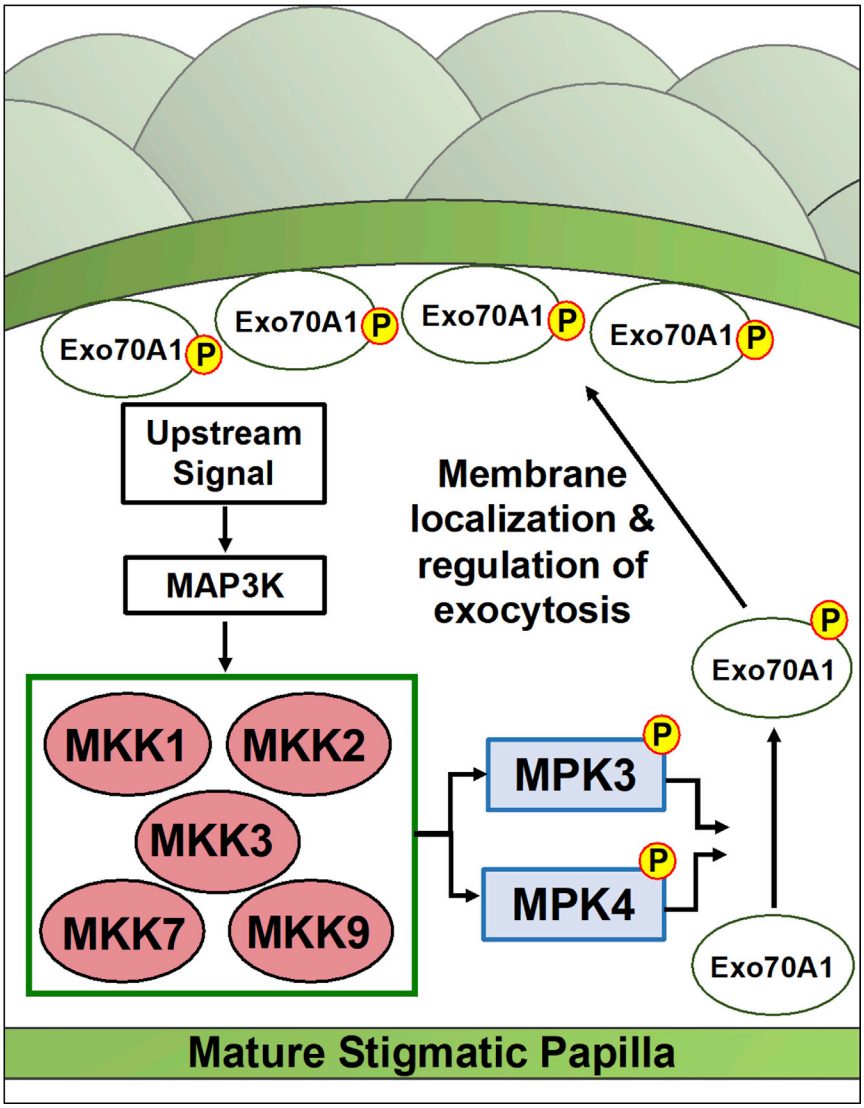

Figure 6. Proposed Model Showing Signaling Events During Papillary Cell Priming for Receiving Pollen in Unpollinated Stage 12 Flowers.

This study shows that serine 328 phosphorylation of Exo70A1 is required for its function throughout the plant. Specifically, in unpollinated stigmatic papillary cells of stage 12 flowers, MAPKs, MPK3, and MPK4 phosphorylate Exo70A1 to trigger its localization to the plasma membrane, where it regulates exocytosis to facilitate successful pollination.

liquid nitrogen and stored at −80°C until further analysis. For protein extraction, stigmas were grounded in extraction buffer (100 mM Hepes [pH 7.5], 5 mM EDTA, 5 mM EGTA, 10 mM DTT, 10 mM Na_3VO_4, 10 mM NaF, 50 mM β-glycerophosphate, 1 mM phenylmethylsulfonyl fluoride, and protease inhibitor cocktail [Roche]), centrifuged at 13 000 rpm for 15 min at 4°C to pellet the debris. Extracts containing 5 μg of proteins were resolved on a 10% SDS gel embedded with 250 μg/ml of myelin basic protein. SDS was removed by washing the gel with washing buffer (25 mM Tris [pH 7.5], 0.5 mM DTT, 0.1 mM Na_3VO_4, 5 mM NaF, 0.5 mg/ml BSA, 0.1% Triton X-100 [v/v]) three times at room temperature. The gel was then incubated in renaturation buffer (25 mM Tris [pH 7.5], 1 mM DTT, 0.1 mM Na_3VO_4, and 5 mM NaF) overnight at 4°C with three buffer changes. The gel was then transferred to reaction buffer (25 mM Tris [pH 7.5], 2 mM EGTA, 12 mM $MgCl_2$, 1 mM DTT, 0.1 mM Na_3VO_4, and 200 nM ATP) for 30 min at room temperature followed by 60 min incubation in same reaction buffer with 25 μCi γ-^{32}P (specific activity 3000 Ci/mmol). After incubation gel was transferred to 5% trichloroacetic acid (w/v) and 1% NaPPi (w/v) to stop the reaction. The gel was washed for five times in 1 h to remove unincorporated γ-^{32}P followed by drying in a GelAir dryer for 90 min with heating and 30 min at room temperature. The dried gel was subjected to phospho-imaging screen to detect kinase activity.

In Vitro Kinase Assay

Recombinant purified proteins were used for *in vitro* phosphorylation assay. Recombinant 6×HIS-MPK4 (5 μg) was activated with GST-CAKK1 (1 μg) in phosphorylation reaction buffer (20 mM Hepes [pH 7.5], 10 mM $MgCl_2$, and 1 mM DTT) at 28°C for 1.5 h. Activated proteins were then used to phosphorylate recombinant GST-Exo70A1 (5 and 10 μg) in the same reaction buffer with the addition of 25 μM ATP and γ-^{32}P-ATP (1 μCi per reaction specific activity 3000 Ci/mmol) for 30 min at 28°C. The reaction was stopped by adding 6× SDS loading buffer. Reaction mixture was resolved on 10% SDS gel followed by staining and destaining of gels to visualize proteins. The gel was air dried for 90 min with heating and 30 min at room temperature. Phosphorylated GST-Exo70A1 was visualized by autoradiography.

Dot Blot Analysis

AtExo70A1 short peptides from residue 323 to 335 (AR***S***KR***S***PEKLFVL and AR***S***KR***A***PEKLFVL) were synthesized from GL Biochem (Shanghai, China). Peptides were dissolved in 1× PBS (pH 7.0–7.5) and immobilized on PVDF membrane in various concentrations followed by air drying for 2 h. Membranes were blocked with 5% BSA (w/v) for 1 h and incubated in kinase assay buffer (20 mM Hepes [pH 7.5] and 10 mM $MgCl_2$) at 30°C with either CAKK1-6×HIS-MPK4 or CAKK7-6×HIS-MPK3 in the presence of phosphatase inhibitor (25 mM NaF, 0.2 M NaPPi, and 2 mM Na_3VO_4). Membranes were probed with anti-pSer antibody 1:5000 (ab9332, Abcam) in the presence of phosphatase inhibitors (25 mM NaF and 1 mM Na_3VO_4) followed by goat anti-rabbit secondary antibody and development with ECL (Amersham).

Aniline Blue Assay

Aniline blue assay was performed as described earlier (Samuel et al., 2009). In the case of inhibitor analysis, Col-0 stigmas were incubated in U0126 overnight and pollinated for 4 h with Col-0 pollen grains. *Arabidopsis* Col-0 and mutants were allowed to naturally pollinate and stigmas were collected 4 h after flower opening, fixed in 3:1 ethanol:glacial acetic acid for 30 min followed by 1 h incubation in 1 N NaOH at 60°C. Stigmas were then washed with distilled water for three times and stained for 30 min with basic aniline blue (0.1% aniline blue in 0.1 M K_3PO_4). Stained stigmas were mounted in 50% glycerol and pollen attachment and pollen tube germination were observed in the blue channel under Leica DMR epifluorescence microscope.

Reverse Transcriptase qPCR

Stage 12 stigmas from Col-0 and the various mutants were collected in liquid nitrogen and stored at −80°C until further analysis. Total RNA was

extracted from these stigmas using RNeasy columns with plant RNA extraction aid (QIAGEN RNeasy Mini Kit) according to manufacturer's instructions. RNA was quantified using a NanoDrop spectrophotometer and RNA integrity was further confirmed by resolving on an agarose gel. Total RNA was treated with DNase I (Thermo Scientific Bio) and reverse transcription was performed with 500 ng of RNA using superscript II (Invitrogen) according to the manufacturer's instructions. qPCRs were performed with SYBR Green dye in a StepOnePlus PCR detector (Applied Biosystems). PCR amplification was performed for 40 cycles at 95°C for 3 s and 60°C for 30 s with a preceding initial enzyme activation of 20 s at 95°C. Relative expression levels were calculated using the delta-delta-Ct method. *UBQ10* was used as endogenous control for all samples. Primers used for qPCR for *MPK3*, *MPK4*, *MKK1*, *MKK2*, *MKK3*, *MKK7*, and *MKK9* are shown in Supplemental Table 5.

Confocal Microscopy

A Leica SP5 laser confocal microscope was used for Exo70A1 localization studies. Images were acquired with 40× oil-immersion objective and the highly sensitive Leica HyD detector. *Arabidopsis* 35S::YFP-Exo70A1, 35S::YFP-Exo70A1(S328A), and 35S::YFP-Exo70A1(S328D) stage 12 stigmas were mounted in 50% glycerol and subjected to confocal imaging. To capture the YFP signal, stigmas were scanned using an argon laser (excitation 476 nm, emission 490–535 nm). Autofluorescence was detected between 590 and 720 nm emission wavelength and merged images were generated by combining both channels. At least three different transgenic lines were examined for each construct.

SUPPLEMENTAL INFORMATION

Supplemental Information can be found online at *Molecular Plant Online*.

FUNDING

This work was supported by Natural Sciences and Engineering Research Council of Canada funding for M.A.S.

AUTHOR CONTRIBUTIONS

M.J. and M.A.S. initiated the project. M.J., S.S., and M.A.S. designed the research. M.J., S.S., K.A., and M.A.S. performed all the experiments. M.J. and M.A.S. analyzed the data and wrote the manuscript. All authors were involved in manuscript discussions and commented on the manuscript.

ACKNOWLEDGMENTS

We thank Dr. Brian Ellis (UBC) for sharing recombinant MPK and MKK constructs. We thank Dr. Douglas Muench for the epi-fluorescence microscope facility. No conflict of interest declared.

Received: March 19, 2020
Revised: June 25, 2020
Accepted: August 28, 2020
Published: September 2, 2020

REFERENCES

Bush, S.M., and Krysan, P.J. (2007). Mutational evidence that the *Arabidopsis* MAP kinase MPK6 is involved in anther, inflorescence, and embryo development. J. Exp. Bot. **58**:2181–2191.

Clough, S.J., and Bent, A.F. (1998). Floral dip: a simplified method for *Agrobacterium*-mediated transformation of *Arabidopsis thaliana*. Plant J. **16**:735–743.

Cullen, P.J., and Lockyer, P.J. (2002). Integration of calcium and Ras signalling. Nat. Rev. Mol. Cell Biol. **3**:339–348.

Desikan, R., Hancock, J.T., Ichimura, K., Shinozaki, K., and Neill, S.J. (2001). Harpin induces activation of the *Arabidopsis* mitogen-activated protein kinases AtMPK4 and AtMPK6. Plant Physiol. **126**:1579–1587.

Dickinson, H. (1995). Dry stigmas, water and self-incompatibility in *Brassica*. Sex. Plant Reprod. **8**:1–10.

Dóczi, R., ökrész, L., Romero, A.E., Paccanaro, A., and Bögre, L. (2012). Exploring the evolutionary path of plant MAPK networks. Trends Plant Sci. **17**:518–525.

Doucet, J., Lee, H.K., and Goring, D.R. (2016). Pollen acceptance or rejection: a tale of two pathways. Trends Plant Sci. **21**:1058–1067.

Drdová, E.J., Synek, L., Pečenková, T., Hála, M., Kulich, I., Fowler, J.E., Murphy, A.S., and Žárský, V. (2013). The exocyst complex contributes to PIN auxin efflux carrier recycling and polar auxin transport in *Arabidopsis*. Plant J. **73**:709–719.

Elleman, C.J., Franklin-Tong, V., and Dickinson, H.G. (1992). Pollination in species with dry stigmas: the nature of the early stigmatic response and the pathway taken by pollen tubes. New Phytol. **121**:413–424.

Favata, M.F., Horiuchi, K.Y., Manos, E.J., Daulerio, A.J., Stradley, D.A., Feeser, W.S., Van Dyk, D.E., Pitts, W.J., Earl, R.A., Hobbs, F., et al. (1998). Identification of a novel inhibitor of mitogen-activated protein kinase kinase. J. Biol. Chem. **273**:18623–18632.

Fendrych, M., Synek, L., Pečenková, T., Drdová, E.J., Sekereš, J., De Rycke, R., Nowack, M.K., and Žárský, V. (2013). Visualization of the exocyst complex dynamics at the plasma membrane of *Arabidopsis thaliana*. Mol. Biol. Cell **24**:510–520.

Frei dit Frey, N., Garcia, A.V., Bigeard, J., Zaag, R., Bueso, E., Garmier, M., Pateyron, S., De Tauzia-Moreau, M.L., Brunaud, V., Balzergue, S., et al. (2014). Functional analysis of *Arabidopsis* immune-related MAPKs uncovers a role for MPK3 as negative regulator of inducible defences. Genome Biol. **15**:R87.

Galletti, R., Ferrari, S., and de Lorenzo, G. (2011). *Arabidopsis* MPK3 and MPK6 play different roles in basal and oligogalacturonide- or flagellin-induced resistance against *Botrytis cinerea*. Plant Physiol. **157**:804–814.

Gao, M., Liu, J., Bi, D., Zhang, Z., Cheng, F., Chen, S., and Zhang, Y. (2008). MEKK1, MKK1/MKK2 and MPK4 function together in a mitogen-activated protein kinase cascade to regulate innate immunity in plants. Cell Res. **18**:1190–1198.

Guan, Y., Lu, J., Xu, J., McClure, B., and Zhang, S. (2014). Two mitogen-activated protein kinases, MPK3 and MPK6, are required for funicular guidance of pollen tubes in *Arabidopsis*. Plant Physiol. **165**:528–533.

Hord, C.L.H., Sun, Y.J., Pillitteri, L.J., Torii, K.U., Wang, H., Zhang, S., and Ma, H. (2008). Regulation of *Arabidopsis* early anther development by the mitogen-activated protein kinases, MPK3 and MPK6, and the ERECTA and related receptor-like kinases. Mol. Plant **1**:645–658.

Ichimura, K., Mizoguchi, T., Yoshida, R., Yuasa, T., and Shinozaki, K. (2000). Various abiotic stresses rapidly activate *Arabidopsis* MAP kinases ATMPK4 and ATMPK6. Plant J. **24**:655–665.

Ichimura, K., Shinozaki, K., Tena, G., Sheen, J., Henry, Y., Champion, A., Kreis, M., Zhang, S., Hirt, H., Wilson, C., et al. (2002). Mitogen-activated protein kinase cascades in plants: a new nomenclature. Trends Plant Sci. **7**:301–308.

Iwano, M., Shiba, H., Miwa, T., Che, F.S., Takayama, S., Nagai, T., Miyawaki, A., and Isogai, A. (2004). Ca^{2+} dynamics in a pollen grain and papilla cell during pollination of *Arabidopsis*. Plant Physiol. **136**:3562–3571.

Jin, S.L., Kyung, W.H., Bhargava, A., and Ellis, B.E. (2008). Comprehensive analysis of protein-protein interactions between *Arabidopsis* MAPKs and MAPK kinases helps define potential MAPK signalling modules. Plant Signal. Behav. **3**:1037–1041.

Kong, Q., Qu, N., Gao, M., Zhang, Z., Ding, X., Yang, F., Li, Y., Dong, O.X., Chen, S., Li, X., et al. (2012). The MEKK1-MKK1/MKK2-MPK4 kinase cascade negatively regulates immunity mediated by a mitogen-activated protein kinase kinase kinase in *Arabidopsis*. Plant Cell **24**:2225–2236.

Kovtun, Y., Chiu, W.L., Tena, G., and Sheen, J. (2000). Functional analysis of oxidative stress-activated mitogen-activated protein kinase cascade in plants. Proc. Natl. Acad. Sci. U S A **97**:2940–2945.

Lampard, G.R., MacAlister, C.A., and Bergmann, D.C. (2008). *Arabidopsis* stomatal initiation is controlled by MAPK-mediated regulation of the bHLH SPEECHLESS. Science **322**:1113–1116.

Li, S., Šamaj, J., and Franklin-Tong, V.E. (2007). A mitogen-activated protein kinase signals to programmed cell death induced by self-incompatibility in *Papaver* pollen. Plant Physiol. **145**:236–245.

Lu, H., Liu, S., Zhang, G., Kwong, L.N., Zhu, Y., Miller, J.P., Hu, Y., Zhong, W., Zeng, J., Wu, L., et al. (2016). Oncogenic BRAF-mediated melanoma cell invasion. Cell Rep. **15**:2012–2024.

McInnis, S.M., Desikan, R., Hancock, J.T., and Hiscock, S.J. (2006). Production of reactive oxygen species and reactive nitrogen species by angiosperm stigmas and pollen: potential signalling crosstalk? New Phytol. **172**:221–228.

Meng, X., Wang, H., He, Y., Liu, Y., Walker, J.C., Torii, K.U., and Zhang, S. (2013). A MAPK cascade downstream of ERECTA receptor-like protein kinase regulates *Arabidopsis* inflorescence architecture by promoting localized cell proliferation. Plant Cell **24**:4948–4960.

Miles, G.P., Samuel, M.A., Zhang, Y., and Ellis, B.E. (2005). RNA interference-based (RNAi) suppression of AtMPK6, an *Arabidopsis* mitogen-activated protein kinase, results in hypersensitivity to ozone and misregulation of AtMPK3. Environ. Pollut. **138**:230–237.

Petersen, M., Brodersen, P., Naested, H., Andreasson, E., Lindhart, U., Johansen, B., Nielsen, H.B., Lacy, M., Austin, M.J., Parker, J.E., et al. (2000). *Arabidopsis* MAP kinase 4 negatively regulates systemic acquired resistance. Cell **103**:1111–1120.

Pitzschke, A., Schikora, A., and Hirt, H. (2009). MAPK cascade signalling networks in plant defence. Curr. Opin. Plant Biol. **12**:421–426.

Popescu, S.C., Popescu, G.V., Bachan, S., Zhang, Z., Gerstein, M., Snyder, M., and Dinesh-Kumar, S.P. (2009). MAPK target networks in *Arabidopsis thaliana* revealed using functional protein microarrays. Genes Dev. **23**:80–92.

Ren, J., and Guo, W. (2012). ERK1/2 regulate exocytosis through direct phosphorylation of the exocyst component Exo70. Dev. Cell **22**:967–978.

Rodriguez, M.C.S., Petersen, M., and Mundy, J. (2010). Mitogen-activated protein kinase signaling in plants. Annu. Rev. Plant Biol. **61**:621–649.

Safavian, D., and Goring, D.R. (2013). Secretory activity is rapidly induced in stigmatic papillae by compatible pollen, but inhibited for self-incompatible pollen in the brassicaceae. PLoS One **8**:1–13.

Safavian, D., Zayed, Y., Indriolo, E., Chapman, L., Ahmed, A., and Goring, D.R. (2015). RNA silencing of exocyst genes in the stigma impairs the acceptance of compatible pollen in *Arabidopsis*. Plant Physiol. **169**:2526–2538.

Samuel, M.A., Miles, G.P., and Ellis, B.E. (2000). Ozone treatment rapidly activates MAP kinase signalling in plants. Plant J. **22**:367–376.

Samuel, M.A., Chong, Y.T., Haasen, K.E., Aldea-Brydges, M.G., Stone, S.L., and Goring, D.R. (2009). Cellular pathways regulating responses to compatible and self-incompatible pollen in *Brassica* and *Arabidopsis* stigmas intersect at Exo70A1, a putative component of the exocyst complex. Plant Cell **21**:2655–2671.

Samuel, M.A., Tang, W., Jamshed, M., Northey, J., Smith, D., Siu, M., Muench, D.G., Wang, Z., and Daphne, R. (2011). Proteomic analysis of *Brassica* stigmatic proteins following the self-incompatibility reaction reveals a role for microtubule dynamics during pollen responses. Proteomic Anal. **10**:1–13.

Sankaranarayanan, S., Jamshed, M., and Samuel, M.A. (2015). Degradation of glyoxalase I in *Brassica napus* stigma leads to self-incompatibility response. Nat. Plants **1**:1–7.

Sun, T., Nitta, Y., Zhang, Q., Wu, D., Tian, H., Lee, J.S., and Zhang, Y. (2018). Antagonistic interactions between two MAP kinase cascades in plant development and immune signaling. EMBO Rep. **19**:e45324.

Sung, K.C., Larue, C.T., Chevalier, D., Wang, H., Jinn, T.L., Zhang, S., and Walker, J.C. (2008). Regulation of floral organ abscission in *Arabidopsis thaliana*. Proc. Natl. Acad. Sci. U S A **112**:2906–2911.

Synek, L., Schlager, N., Eliáš, M., Quentin, M., Hauser, M.T., and Žárský, V. (2006). AtEXO70A1, a member of a family of putative exocyst subunits specifically expanded in land plants, is important for polar growth and plant development. Plant J. **48**:54–72.

Takahashi, Y., Soyano, T., Kosetsu, K., Sasabe, M., and Machida, Y. (2010). HINKEL kinesin, ANP MAPKKKs and MKK6/ANQ MAPKK, which phosphorylates and activates MPK4 MAPK, constitute a pathway that is required for cytokinesis in *Arabidopsis thaliana*. Plant Cell Physiol. **51**:1766–1776.

Wang, H., Ngwenyama, N., Liu, Y., Walker, J.C., and Zhang, S. (2007). Stomatal development and patterning are regulated by environmentally responsive mitogen-activated protein kinases in *Arabidopsis*. Plant Cell **19**:63–73.

Wang, H., Liu, Y., Bruffett, K., Lee, J., Hause, G., Walker, J.C., and Zhang, S. (2008). Haplo-insufficiency of MPK3 in MPK6 mutant background uncovers a novel function of these two MAPKs in *Arabidopsis* ovule development. Plant Cell **20**:602–613.

Wu, C., Tan, L., van Hooren, M., Tan, X., Liu, F., Li, Y., Zhao, Y., Li, B., Rui, Q., Munnik, T., et al. (2017). *Arabidopsis* EXO70A1 recruits Patellin3 to the cell membrane independent of its role as an exocyst subunit. J. Integr. Plant Biol. **59**:851–865.

Xu, J., and Zhang, S. (2015). Mitogen-activated protein kinase cascades in signaling plant growth and development. Trends Plant Sci. **20**:56–64.

Zhang, J., Gao, J., Zhu, Z., Song, Y., Wang, X., Wang, X., and Zhou, X. (2020). MKK4/MKK5-MPK1/MPK2 cascade mediates SA-activated leaf senescence via phosphorylation of NPR1 in *Arabidopsis*. Plant Mol. Biol. **102**:463–475.